SEISMIC SSSI EFFECTS FOR DEEPLY EMBEDDED SMR WITH SC/RC WALLS UNDER SEVERE EARTHQUAKES IN NONUNIFORM SOILS

Dan M. Ghiocel[1], Yasuo Nitta[2] and Ryosuke Ikeda[3] and Tomohiro Horiguchi. [4]

[1] President, Ghiocel Predictive Technologies, Inc., New York, USA (dan.ghiocel@ghiocel-tech.com)
[2] Senior Engineer, SHIMIZU Corporation, Tokyo, Japan (nitta_y@shimz.co.jp)
[3] General Manager, SHIMIZU Corporation, Tokyo, Japan (ikedar@shimz.co.jp)
[4] Structural Engineer, Terrabyte Corporation, Tokyo, Japan (tomohiro.horiguchi@terrabyte.co.jp)

ABSTRACT

The paper investigates the dynamic behavior of deeply embedded SMR structure with mixed steel-composite concrete (SC) walls and reinforced concrete (RC) walls under severe earthquakes. Since the neighboring AB building is at a small separation distance of 2.5 ft from SMR, the effects of the structure-soil-structure interaction (SSSI) were included. The structural SC wall modeling is considered in accordance with both the US and Japan standards, including AISC N690-18 and ACI 318-18/349-19 standards in US and JEAC 4618-2009 and JEAC 4601-2015 standards in Japan. The nonlinear structure SSI analysis is based on an efficient iterative hybrid approach which couples the equivalent-linear complex frequency-domain overall SSI analysis with a nonlinear time-domain superstructure analysis. The SMR embedded wall-soil interface is considered as a smooth, no friction interface for the linear SSI analyses as required by the AISC N690 standard, and as a nonlinear friction slipping interface for the nonlinear structure SSI analysis as required by the JEAC 4618-2009 standard. The paper includes a description of the SC wall modeling in US and Japanese standards, and a set of comparative results obtained using the US and Japanese standards. Some visible differences are noted between the SSSI analysis results using the two different standard requirements. The ACS SASSI Option NON software was used for this study.

DESCRIPTION OF THE SSSI MODEL INCLUDING SMR SC AND AB RC STRUCTURES

The overall seismic SSSI model is shown in Figure 1, while the SMR configuration is detailed in Figure 2. The SMR structure includes a mix of SC and RC walls; the external and internal walls are SC walls, while the reactor vessel containment vessel (RVC) is a cylindrical RC wall. The SMR structure has a horizontal section size of 100 ft by 100 ft, and a total vertical size of 162.50 ft including an embedment of 118 ft and a super-structure with a height of 44.50 ft above ground. The standalone SMR SSI model has a total of 30,924 nodes including 15,780 excavation nodes. The AB is a reinforced concrete (RC) structure has a horizontal size of 196 ft x 80 ft and an embedment of 21.4 ft. The AB roof level is at 102.5 ft above the ground level. The ACS SASSI SSSI model has a total number of 42,735 nodes including 22,492 excavation nodes. The SMR excavation depth includes 30 embedment layers down to 118 ft depth.

Two specific-site conditions were considered (Ghiocel and Todorovski, 2024): 1) Site 1, a deep soft soil deposit, and 2) Site 2, a shallow firm soil layer above a hardrock formation. It should be noted that for Site 2, the SMR foundation depth goes inside the hard-rock formation with a Vs of @ 6500 fps.

The seismic input motion frequency content corresponded to the specific-site surface GRS for the two site soil conditions. The maximum ground acceleration was assumed to be 0.30g for the Design-Basis Earthquake (DBE) level and 0.60g for the Beyond Design-Basis Earthquake (BDBE) level. The linear SSI analysis per AISC N690/ASCE 4 and nonlinear structure SSI analysis per JEAC 4601/4618 were performed for both the 0.30g DBE and the 0.60g BDBE inputs.

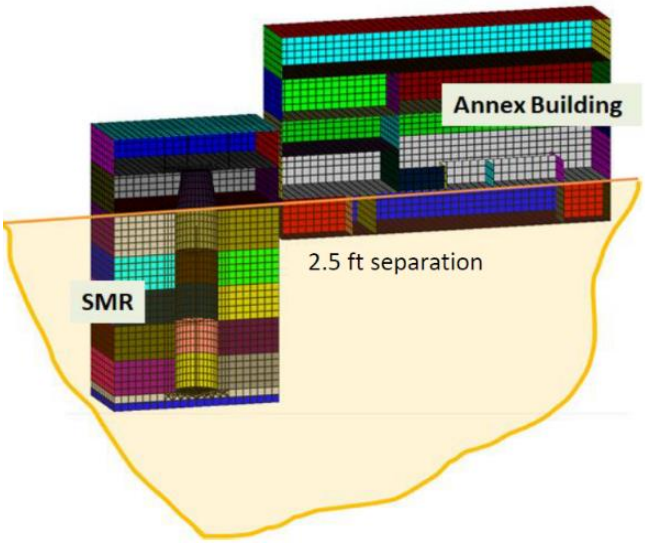

Figure 1 SMR-AB SSSI Model

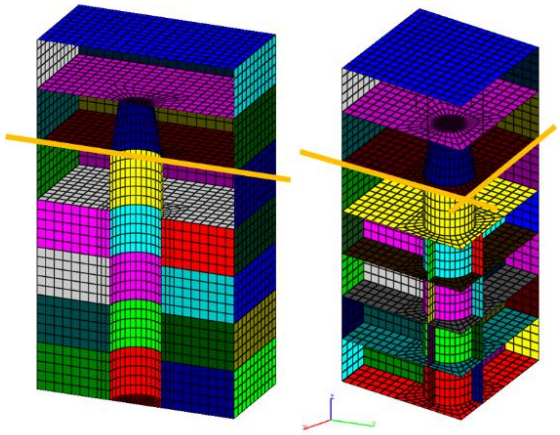

Figure 2 SMR Structure Configuration

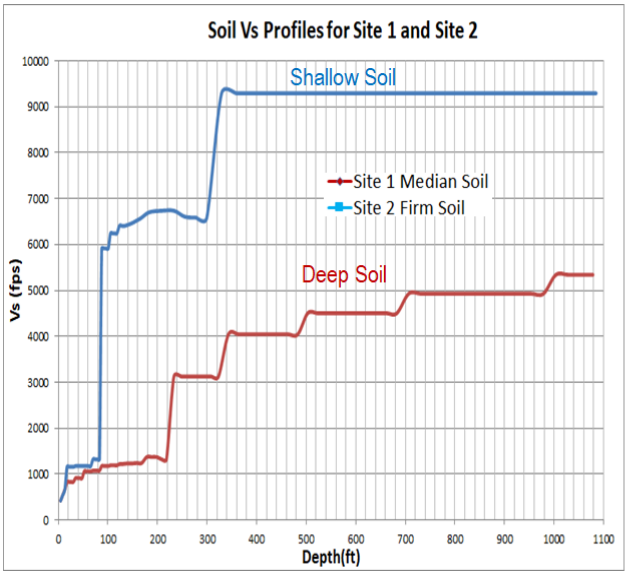

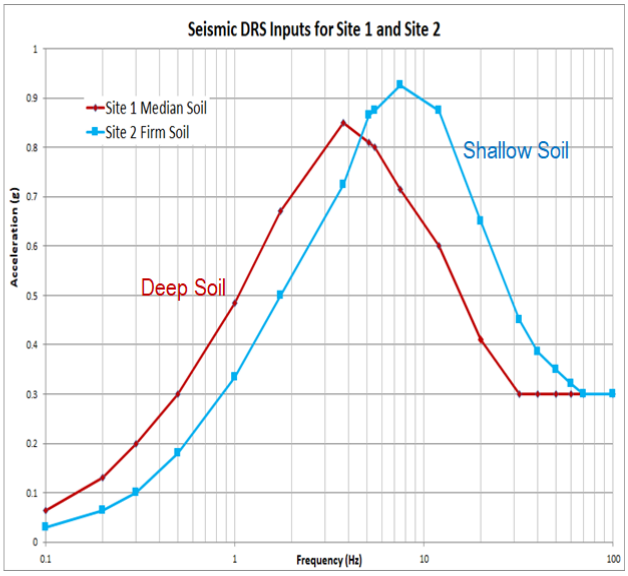

Figure 3 The Vs Soil Profiles and Input GRS at Ground Surface for Two Site Conditions, Site 1 and Site 2

SMR SC WALL MODELING PER US AISC N690 AND JAPANESE JEAC 4618 STANDARDS

It should be noted that between the AISC N690 standard and the JEAC 4618 standard there is a significant discrepancy between the assumptions for the seismic SSI modeling and analysis. The US standard requires linear SSI analysis for the SC wall structures, while Japanese standard requires nonlinear structure SSI analysis for the SC wall structures.

The AISC N690 standard requires the use of the effective stiffnesses for the SC wall modeling for both uncracked and cracked concrete structures. The effective bending and shear stiffnesses of the SC walls are defined in Section N9.2.2 of AISC N690 based on using modified materials for the uncracked and cracked walls. This material modification addresses the elastic E modulus, the Poisson ratio, the wall thickness and its mass density. Figure 4 summarizes the AISC N690 Section N9 requirements for material modification for the uncracked and cracked SC walls.

$$El_{eff} = E_s I_s + c_2 E_c I_c$$ per AISC N690 equation (Out of plane bending stiffness)

Uncracked Concrete

$$EA_{gross} = E_s A_s + E_c A_c$$

$$T_m = \sqrt{\frac{12 El_{eff}}{EA_{gross}}}$$

$$GA_{uncr} = G_c A_c + G_s A_s$$

$$G_m = \frac{GA_{uncr}}{T_m}$$

Cracked Concrete

$$EA_{eff} = E_s A_s + \frac{E_c A_c}{2}$$

$$T_m = \sqrt{\frac{12 El_{eff}}{EA_{eff}}}$$

$$GA_{cr} = 0.5 * \rho bar^{-0.42} G_s A_s$$

$$G_m = \frac{GA_{cr}}{T_m}$$

$$\rho bar = \frac{A_s F_y}{31.6 * A_c \sqrt{f'_c}}$$

Modified Material

$$E_m = \frac{12 El_{eff}}{T_m^3}$$

$$V_m = \frac{E_m}{2 * G_m} - 1$$

$$\gamma_m = \frac{\gamma_s * 2T_p + \gamma_c * T_c}{T_m}$$

Figure 4 AISC N690-Based Material Modification for Uncracked and Cracked SC Walls

For the 2ft SMR SC walls, per AISC N690, the modified SC wall equivalent elastic materials for uncracked and cracked SC walls are shown in Figure 5.

Ec	480000	ksf	Ec=w_c^1.5*sqrt(fc)	ksi		
Gc	205128	ksf	Gc=Ec/(2*(1+v))			
Gamma_c (w_c)	0.16	kcf				
Tsc (thick)	2	ft				
2Tp	0.0625	ft	3/8 in			
Ac=Tc = Tsc-2Tp	1.9375	ft				
As =2Tp	0.0625	ft				
Gamma_s	0.49	kcf				
P =2Tp/Tsc	0.03125					
Asc	2					
Tp	0.03125	ft				
Ic	0.6061	ft4	Ic=(Tc^3/12)			
Is	0.0606	ft4	Is=Tp*(Tsc-Tp)^2/2			
c2	0.2259					
Es	4030000	ksf	28000 ksi***			

p1=	0.2624					
f'c =	6	Ksi	864	ksf		
Gs=	10800	ksi	1555200	ksf		
As=	0.0625	ft2				
Ac=	1.9375	ft2				
Fy=	330	N/mm2	47.19	Ksf	47	ksf
robar =	0.019587					
GAcr =	253517	ksf*ft2=ki	CRACKED			
GAuncr =	494636	kip	UNCRRACKED			

UNCRACKED			
	v	0.17	
	Damping	3%	
group 2/3/4/5	EI_eff	309796.9	ksf*ft4
	EA_gross	1181875.0	ksf*ft2
	Gamma_m	0.192	
	Tm	1.774	ft
	Em	666390	ksf
	Gm	278896	ksf
	Vm	0.19469	
EI_eff = Es*Is + c2*Ec*Ic			
EA_gross = Es*As + Ec*Ac			
Tm = sqrt((EI_eff*12)/EA_gross)			
Em = EA_gross/Tm			
Gamma_m=(Gamma_s*2Tp+Gamma_c*Tc)/Tm			
GAuncr = GsAs+GcAc			
CRACKED			
	v	0.17	
	Damping	5%	
group 2/3/4/5	EI_eff	309796.9	ksf*ft4
	EA_eff	716875.0	ksf
	Gamma_m	0.150	
	Tm	2.277	ft
	Em	314801	ksf
	Gm	111327	ksf
	Vm	0.41386	
EI_eff = Es*Is + c2*Ec*Ic/2			
EA_eff = Es*As + (Ec*Ac)/2			
Tm = sqrt((EI_eff*12)/EA_eff)			
Em = EA_eff/Tm3			

Figure 5 Modified Material for Uncracked and Cracked 2ft SC Wall Per AISC N690 Standard

In Figure 5, the left table contains the initial, given concrete and steel material properties, while the right tables shows the modified materials per AISC N690 for uncracked and cracked SC walls, respectively.

Figure 6 shows the uncracked SC wall material modification per the JEAC 4618 standard.

$$E_m = E_c\left(1 + \left(\frac{E_s}{E_c} - 1\right) * p\right)$$

$$G_m = \frac{G_c A_c + G_s A_s}{A_{sc}}$$

$$V_m = \frac{E_m}{2 * G_m} - 1$$

JEAC 4618 SC WALL PARAMETERS		
UNCRACKED SC WALL		
Em=Ec(1+((Es/Ec) -1)*p)	590938	ksf
Gm=(Gc*Ac+Gs*As)/Asc	247318	ksf
v=Em/(2*Gm)-1	0.195	
Gamma (weight)	0.1703125	kcf
thick	2	ft (Exterior Wall)
	2	ft (Interior Wall)
Damping	3%	

Figure 6 Modified Material for Uncracked 2ft SC Walls Per JEAC 4618 Standard

For the cracked SC walls, the JEAC 4618 standard requires including the nonlinear SC wall behaviour. The SC wall input requires the definition of the in-plane shear and bending back-bone curves (BBC) describing the nonlinear restoring shear force-shear strain and bending moment-curvature hysteretic relationships. The JEAC 4618 provides guidance to build the trilinear the shear and bending BBC, including cracking, yielding and ultimate limit state points, as shown in Figure 7.

It should be noted that these BBC curves include three damage limit states, in contrast to the AISC N690 standard that defines only bilinear BBC including cracking and yielding limit states. An important difference is that the JEAC 4618 BBC slopes indicate the tangential stiffness variations to be used for the nonlinear structure analysis, while the AISC N690 BBC slopes indicate the effective secant stiffness to be used for the linear structure analysis. It should be noted that the SC capacities computed by the two standards, however, are basically indentical as shown in Table 1 (Ozaki, 2004, Varma, et al., 2011).

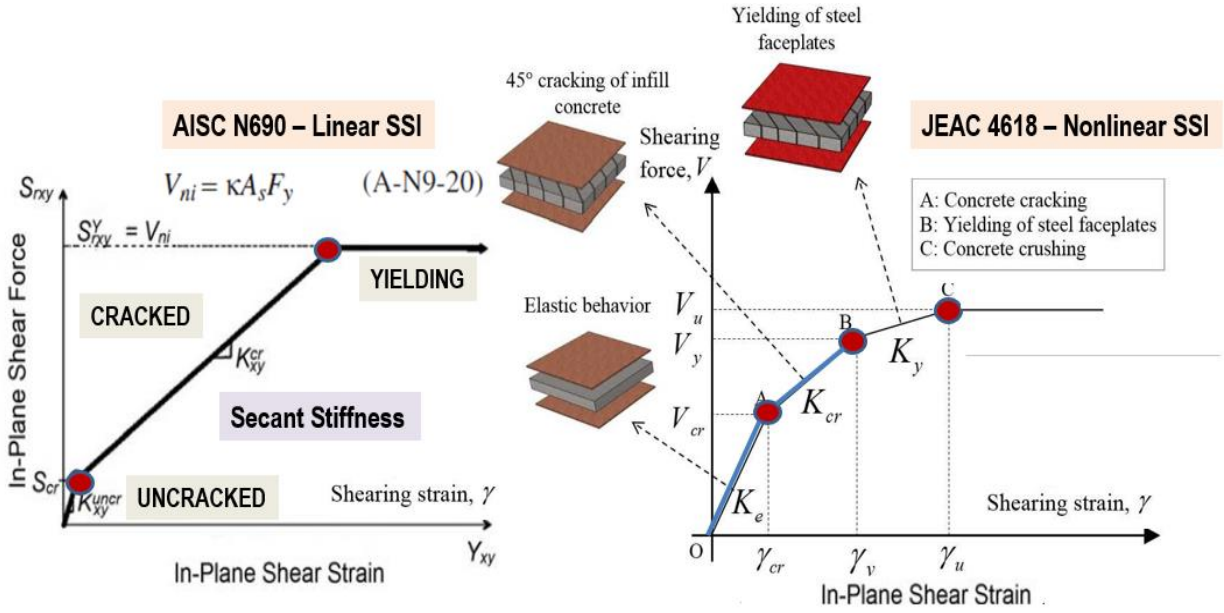

Figure 7 AISC N690 Standard vs. JEAC 4618 In-plane Shear Force-Shear Strain Relationships

Limit state	Shearing force (kips)	Shearing stiffness (kips/rad)
Concrete cracking	$V_{cr} = 0.063\sqrt{f_c'}(A_c + nA_s)$	$K_e = G_s A_s + G_c A_c$
Yielding of the steel faceplates[1]	$V_y = \frac{K_\alpha + K_\beta}{\sqrt{3K_\alpha^2 + K_\beta^2}} A_s f_y$	$K_{cr} = K_\alpha + K_\beta$

Table 1. SC Wall Shear Capacities and Stiffness (Ozaki, 2004, Varma, 2011)

For the AB structure RC wall structural modelling the ACI 318/349 and the JEAC 4601 standard recommendations were followed. The RC wall BBC equations used for the nonlinear structure SSI analysis are based on the JEAC 4601 Appendix 3.7.

The RC/SC wall nonlinear modelling includes two major constitutive components (Figure 8):

1. Back-bone curves (BBC) for shear and bending deformation for each RC wall at each floor level per JEAC 4601 App. 3.7 equations or available experimental tests.

2. Hysteretic models (HM) for the shear and bending deformation effects for each RC wall panel is selected per JEAC 4601 standard recommendations or available experimental tests.

The RC/SC wall BBC and their associated hysteretic models are determined based on the requirements of the JEAC 4601-2015 App.3.7 for RC walls, and JEAC 4618-2009 for SC walls. The "PO shear" and "PODT bending" hysteretic models used for the nonlinear structure SSI analysis are the maximum point-oriented models described in the JEAC 4601 App.3.7.

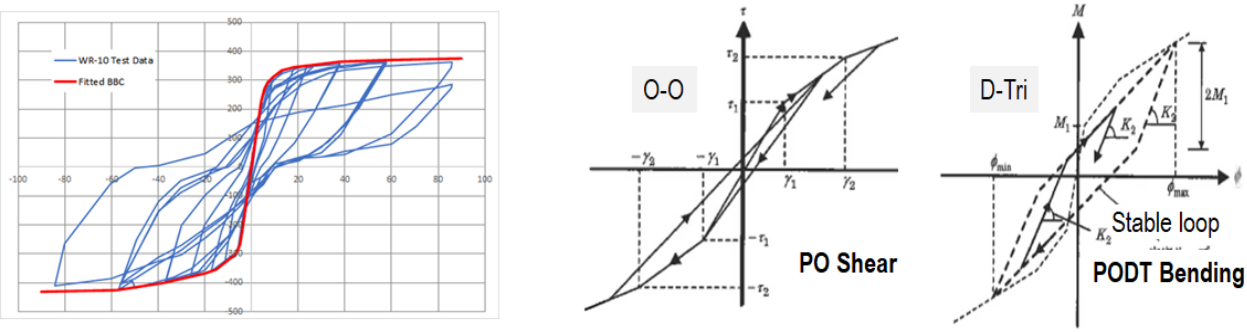

Figure 8 BBC and JEAC 4016 Recommended Maximum Point-Oriented Hysteretic Models

Figure 9 describes the concept of the iterative hybrid frequency-time SSI approach, as implemented in ACS SASSI Option NON for performing efficient nonlinear structure analysis per JEAC 4601 and 4618 standards (Ghiocel, 2022). The hybrid approach includes at each iteration two coupled analysis steps:

Step 1: Perform an *equivalent-linear SSI analysis* in complex frequency via the SASSI approach to compute the structural displacements for each nonlinear SC/RC wall, and then,

Step 2: Perform a *nonlinear time-domain hysteretic analysis* for each SC/RC wall loaded with the SSI displacements from Step 1, to compute the in-plane shear and bending nonlinear wall responses using the *standard-based back-bone curve (BBC) equations* and the *appropriate hysteretic models from the available software library*.

It should be noted that *Step 1* uses the *original, refined FE SSI model* (left plot) while *Step 2* uses a *reduced-order structural model* (right plot) using macro-mechanics models for simulating the SC/RC wall hysteretic behaviour. These macro-mechanics models are called wall "panels" and include all groups of the shell elements defining the SC/RC wall geometry at each floor level (see panels in different colours in the

Figure 9 left plot). Therefore, the Step 2 "true" nonlinear time-domain hysteretic analysis is extremely fast, since is applied to the reduced-size structure model including only the wall panels as macro-mechanics models.

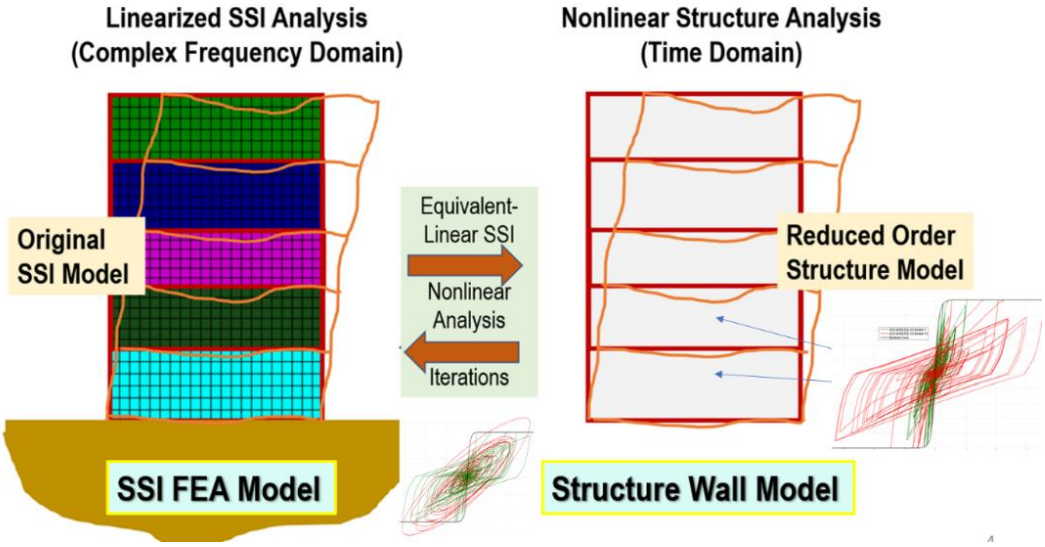

Figure 9 Iterative Hybrid SSI Approach Implemented in ACS SASSI Option NON

The ACS SASSI Option NON was developed in compliance with the US and Japan standards for nonlinear modeling of the SC/RC structures (Ghiocel et al. 2022a, 2022b). Independent verification and validation studies against experimental wall tests and sophisticated nonlinear time domain FE analysis indicated that the iterative equivalent-linearization SSI procedure implemented in the ACS SASSI Option NON provides a reasonable accuracy and a high numerical efficiency (Nitta at al., 2022 Ichihara et al., 2022).

SMR SC AND AB RC WALL NONLINEAR MODELING PER JEAC 4601 AND JEAC 4618

The first step for the nonlinear SC/RC structure modeling is to identify the main resistance walls which are assumed to have behave nonlinearly during the earthquake. For the SC/RC walls, the nonlinear submodels were defined as shown in Figures 10 and 11 for the AB structure and SMR structure, respectively. Each of the two structures has nine nonlinear wall submodels. For each nonlinear wall submodel, the subdivisions of the walls at each floor level define the wall "panels". As shown, these wall panels are numbered bottom-up in sequential order.

Each regular, plane SC/RC wall includes in its cross-section the web and two end flanges, as shown in the two figures. The wall flange widths are computed in accordance with the JEAC 4601-2015 and AIJ RC-2018 requirements (ACI 318 for US practice). For regular SC/RC walls with plane webs, it should be noted that the nonlinear material degradation is assigned differently for the wall webs and wall flanges since the web damage is governed by in-plane shear deformation and the flange damage is governed by bending deformation (GP Technologies, 2023).

If orthotropic material are defined for flanges, then, at each iteration, the interactive bending and shear damage effects can be incorporated into s single physical material model with decoupled shear and bending stiffnesses.

Figure 12 shows the shear and bending BBC computed for the 2ft SMR exterior and interior SC walls described in Figure 11.

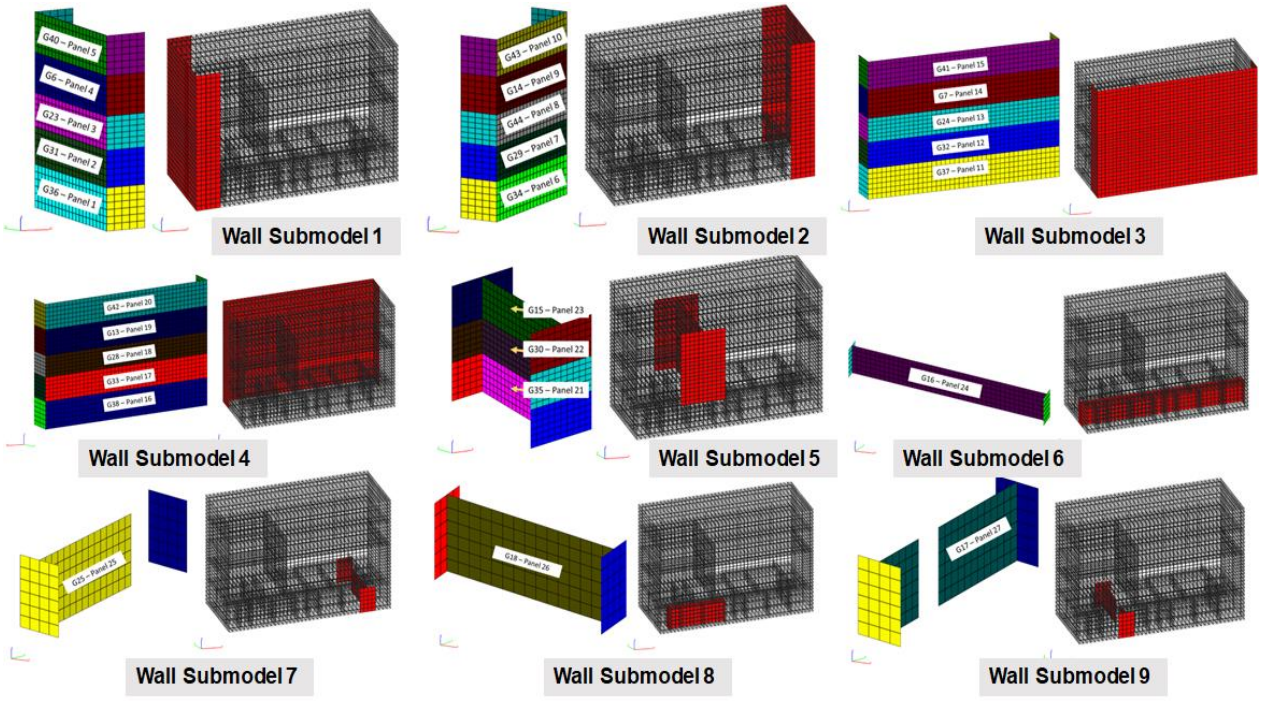

Figure 10 Nonlinear RC Wall Submodels for AB Structure

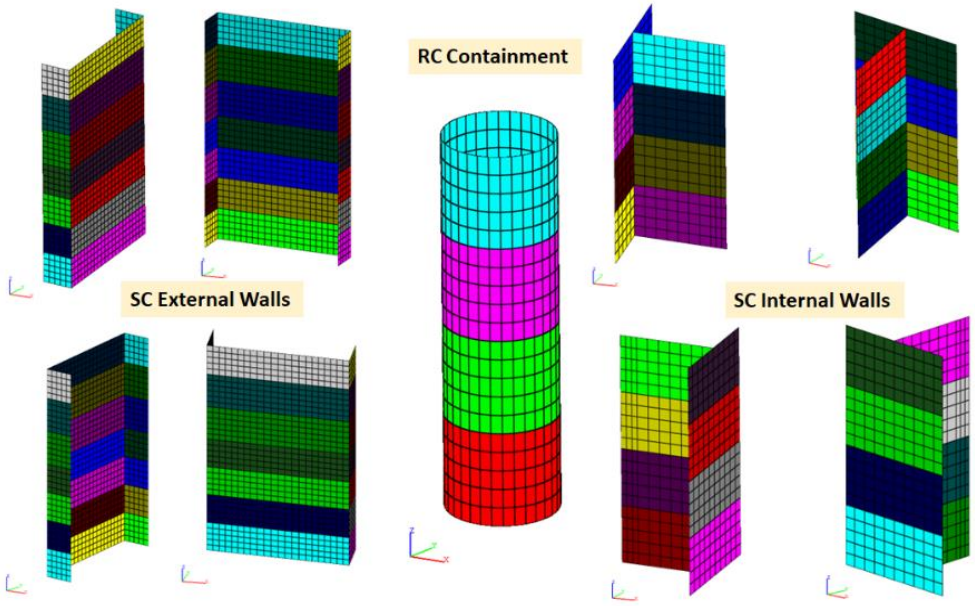

Figure 11 Nonlinear SC/RC Wall Submodels for SMR Structure

In addition to the concrete wall nonlinear behavior, the nonlinear wall-soil interface slipping was also considered for nonlinear structure analysis per JEAC 4601/4618 standards. The nonlinear wall-soil interface was modeled by nonlinear shear springs with bilinear-shaped BBC including a yielding point and an ultimate limit state point. The yielding point corresponds to the start of the wall slipping (Ghiocel, 2022). The shear stress variation with depth was kept at a maximum stress cut-off value of 2 ksf per the API standard recommendations for deep pile and caisson foundations. No wall-soil slipping was considered for the AB structure exterior walls.

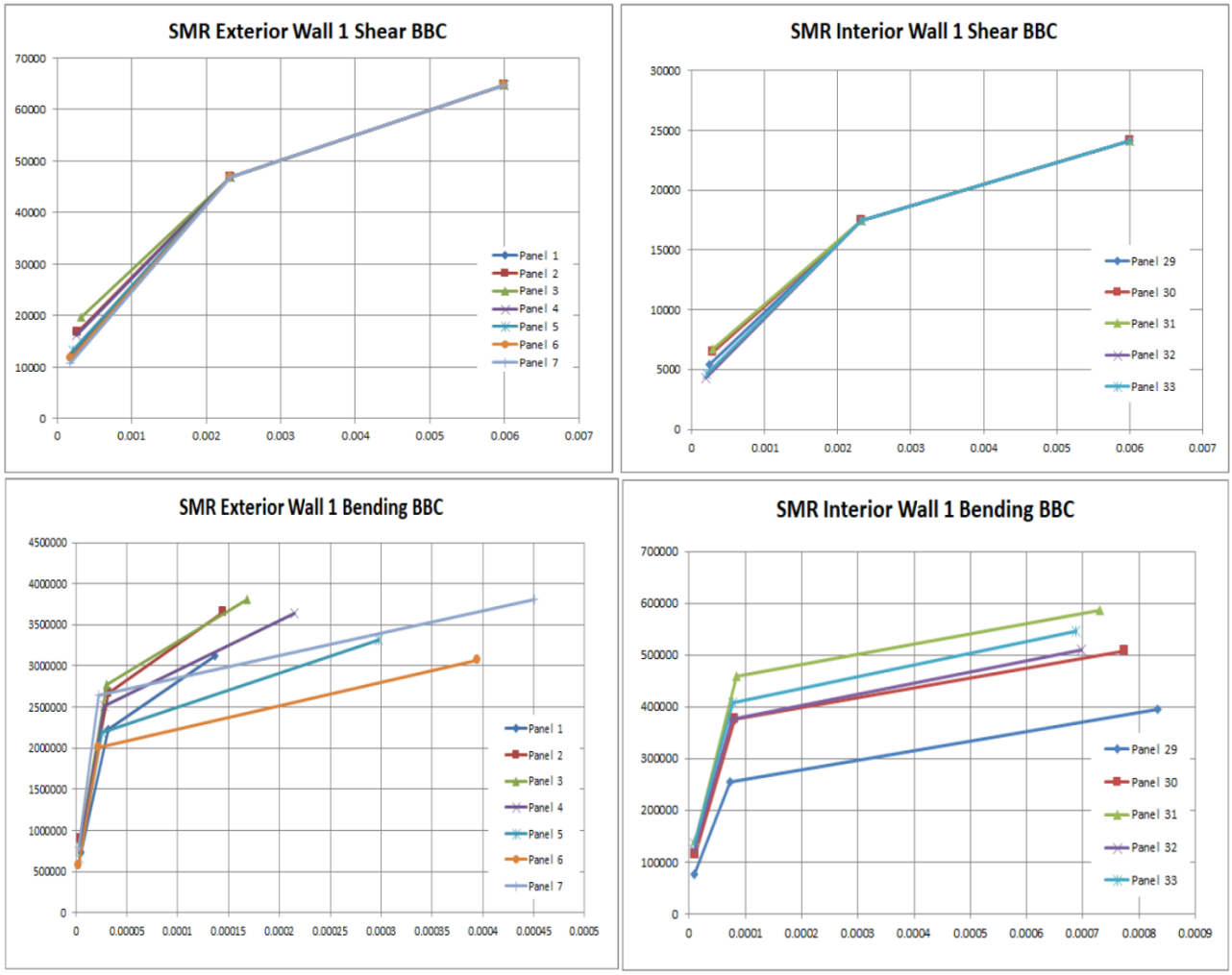

Figure 12 Shear and Bending BBC for Exterior and Interior SC Walls

COMPARATIVE SSSI ANALYSIS RESULTS

Due to the limited space of this paper, only the comparative SSSI results obtained for the 0.60g BDBE input are included herein.

For the linear SSI analysis per AISC N690/ACI 318 only the cracked SC/RC wall models were considered, and the wall-soil interface was assumed to be a smooth interface with very low friction effects included by very soft linear shear stiffness springs.

For the nonlinear SSI analysis per JEAC 4618/4601, nonlinear SC/RC walls are considered. The wall-soil interface was assumed to be a nonlinear friction interface modeled by nonlinear shear stiffness springs with a bilinear hysteretic behaviour (based on the general Massing 4 main rules) that is available in the Option NON model library.

Figures 13 and 14 show the ISRS computed for Site 1 and Site 2 in X-direction (main SSSI coupling direction, longitudinal to AB) using the standalone SMR SSI analysis and the SMR-AB SSSI analysis, respectively. The plotted comparative ISRS results were obtained using linear SSI analysis per AISC N690 with cracked SC/RC walls, and the nonlinear SSI analysis per JEAC 4618/4601 including nonlinear behaviour of the SC/RC walls and the wall-soil slipping interface.

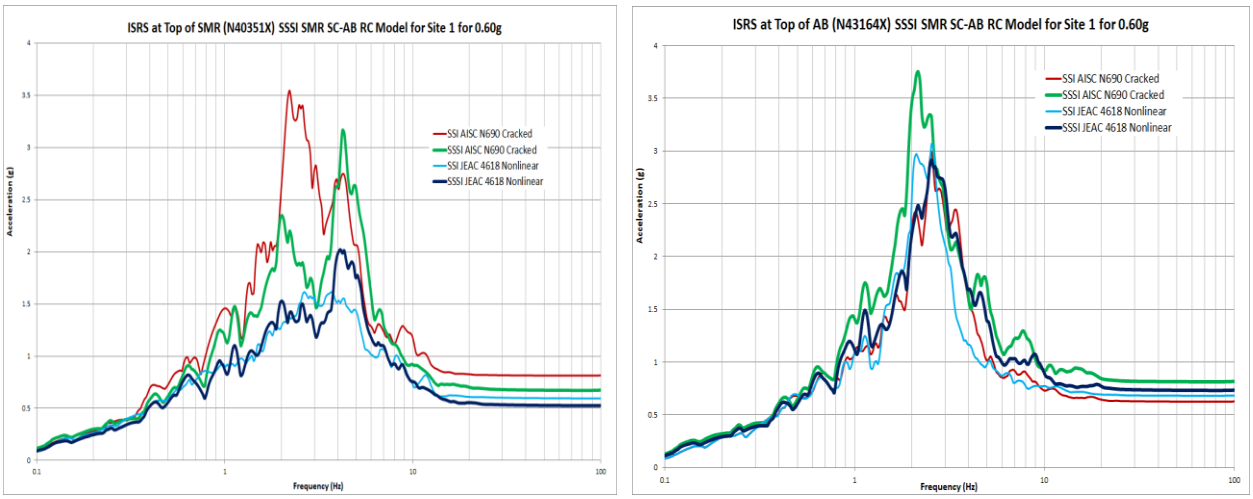

Figure 13 Comparative ISRS at Top of SMR (left) and AB (right) Structures for Site 1 in X-Dir

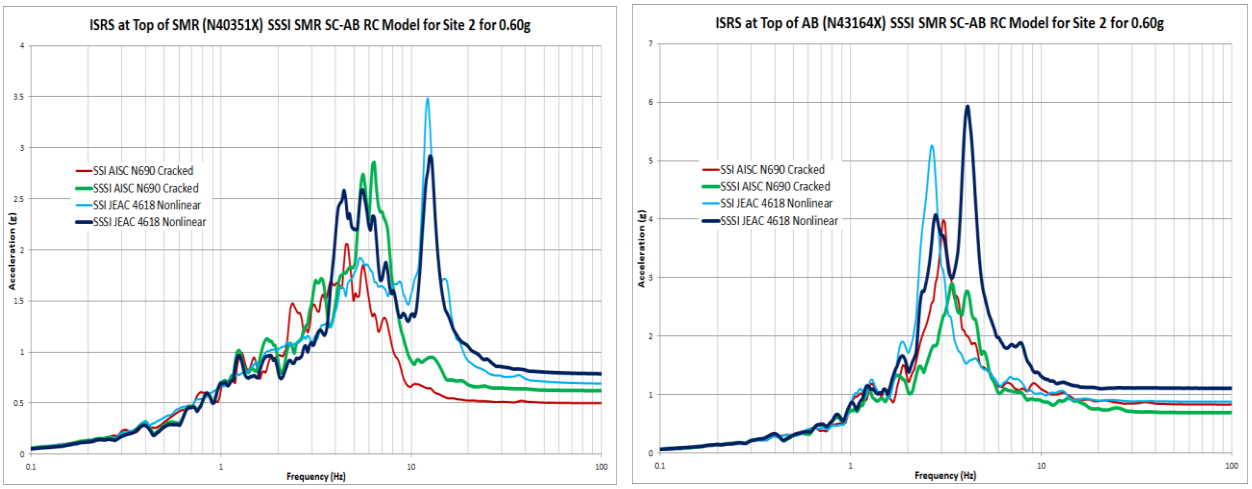

Figure 14 Comparative ISRS at Top of SMR (left) and AB (right) Structures for Site 2 in X-Dir

Figure 13 shows that for Site 1, the SSSI effects on the SMR response in X-direction are favourable for the 1st SSI mode @ 2.5 Hz and unfavourable for the 2nd SSI mode @ 4.5 Hz. However, these SSSI effects are different for the SSI/SSSI analyses per the AISC N690/ASCE 4 and the JEAC 4618/4601, respectively. It should be noted that there are some visible discrepancies between the ISRS results using US and Japan standards. Overall, for SMR structure, the linear SSI results are about twice larger than nonlinear SSI results. In terms of trends, the computed ISRS per the AISC N690/ASCE 4 linear SSI analysis show a large reduction of 35-40% of the 2.5 Hz peak amplitude, while the computed ISRS per the JEAC 4601/4618 nonlinear SSI analysis show a large increase of 33% of the 4.5 Hz peak amplitude. For the AB structure, the linear SSSI effects shows a 2.5 Hz ISRS peak increase by 20-25%, indicating an energy vibration transfer from SMR to AB for the 2.5 Hz coupled SSSI vibration mode.

Figures 14 shows the same location ISRS computed for Site 2. The ISRS discrepancies noted for Site 1 between results of the linear the AISC N690/ASCE 4 linear SSI analysis and the JEAC 4601/4618 nonlinear SSI analysis, are noted again for Site 2. A new noted feature is the 12 Hz SSI mode with a large ISRS peak for the nonlinear SSI/SSSI analysis per the JEAC 4601/4618 standards, which has a very reduced amplitude, but is still visible for the linear SSI/SSSI analysis per AISC N690/ASCE 4 standards. This 12 Hz frequency ISRS peak is most-likely the effect of a higher frequency SSI mode produced by the fact the SMR structure is partially embedded in the hard rock formation with a Vs of about 6500 fps. The SSSI effects amplify by 25-30% the 4-6 Hz range ISRS peak amplitudes for both linear and nonlinear SSI

analyses. For the eAB structure, the SSSI effects show a very large amplification above 100% of the 12 Hz ISRS peak amplitude, and at the same time, the SSSI effects show about 30-35% reductions for the 4-6 Hz range ISRS amplitudes. The Site 2 results indicate energy transfers from SMR to AB for the 12 Hz frequency coupled SSSI vibration mode, and vice-versa from AB to SMR for the 4-6 Hz range SSSI modes.

Figures 15 and 16 shows the SSSI effects on nonlinear in-plane shear forces and bending moments in the SC walls at the bottom floor of the SMR structure.

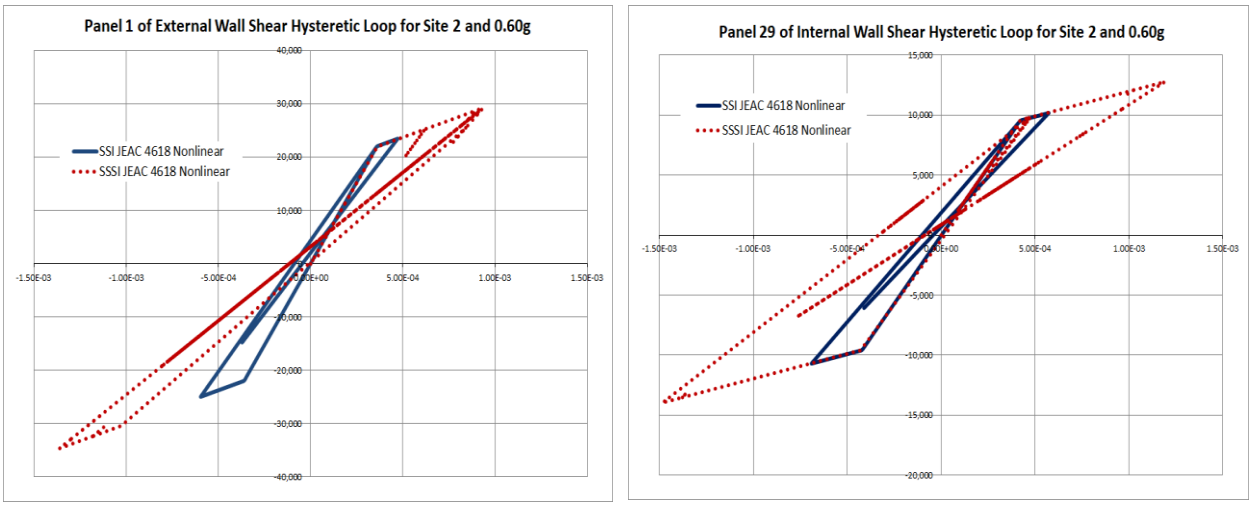

Figure 15 Shear Force Hysteretic Responses in External and Internal SC Walls at Bottom Floor

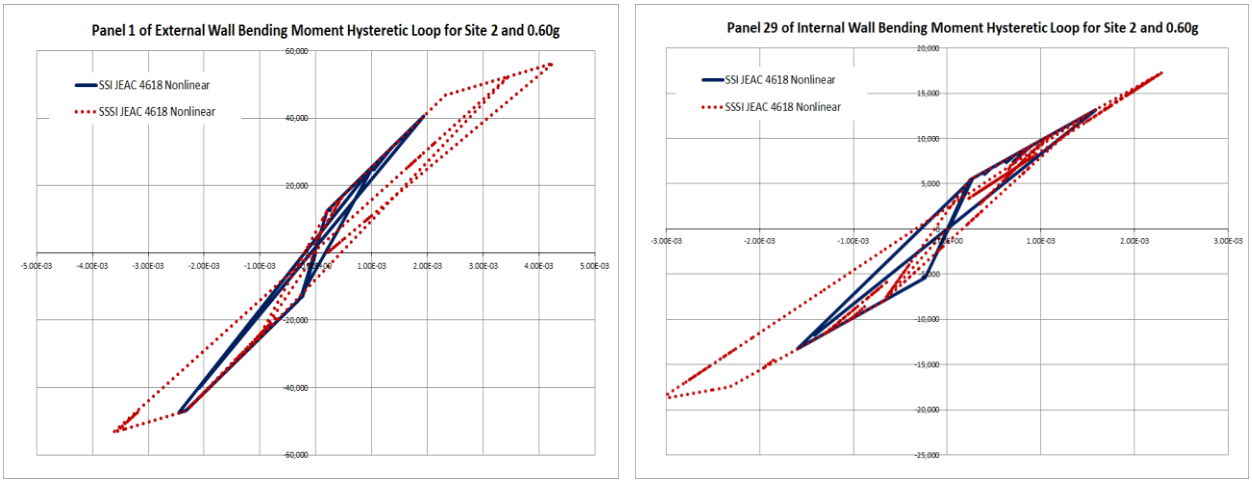

Figure 15 Moment Hysteretic Responses in External and Internal SC Walls at Bottom Floor

Figure 15 compares the computed SSI and SSSI shear force (kips)-shear strain hysteretic loops, while Figure 15 compares the SSI and SSSI nonlinear shear force shear strain hysteretic loops, while Figure 16 compares SSI and SSSI nonlinear bending moment (kips-ft)-curvature(1/m) hysteretic loops. Both figures indicate that the SSSI effects are significant on both the nonlinear wall forces/moments and the shear/bending deformation.

CONCLUDING REMARKS

The paper investigates the SMR-AB SSSI effects for a deeply embedded SMR structure with mixed SC and RC walls and a neighboring AB shearwall subjected to a 0.60g severe earthquake, above the design earthquake level. The SC and RC structural wall modeling is done in compliance with the requirements of the AISC N690-18 and ACI 318-18/349-19 standards in US, and the JEAC 4618-2009 and JEAC 4601-2015 standards in Japan.

For the investigated case studies, significant discrepancies are noted between the SSI and SSSI analysis results using the two country standard requirements. The SSSI effects can largely amplify or reduce the ISRS peak amplitudes, and also increase the structural forces and moments, and displacements, in the deeply embedded SMR structure.

It should be noted that for Site 1, the linear SSI/SSSI analysis per the US standards appears overly conservative for the ISRS results, while for Site 2, the nonlinear SSI/SSSI analysis per the Japan standards appears to be overly conservative.

Detailed explanations and engineering insights on the SMR SC structure modeling are included.

REFERENCES

Ghiocel, D. M. (2022). *Efficient Linear and Nonlinear Seismic SSI Analysis of Deeply Embedded Structures Using Flexible Reduced-Order Modeling (FVROM),* SMiRT26 Conference, Div. 5, Berlin/Potsdam, Germany, July 10-15

Ghiocel, D.M, Nitta, Y., Ikeda, R. and Shono, T (2022a, 2022b). *Seismic Nonlinear SSI Approach Based on Best Practices in US and Japan. Parts 1: Modeling and Part 2: Application*, SMiRT26, Special Session, Berlin, July 10-15

Ghiocel, D.M. and Todorovski, L. (2024) *Seismic SSSI Analysis for Deeply Embedded SMR Structure Founded on Nonuniform Soil Site Conditions,* SMiRT27, Division 5 Special Presentation Session, Yokohama, March 3-8 (submitted).

GP Technologies (2023) *ACS SASSI NQA Version 4.3.6 - An Advanced Computational Software for 3D Dynamic Analysis Including Soil-Structure Interaction, Including Options A-AA and NON Advanced,* GP Technologies, Inc., User Manuals, Revision 8, New York, USA

Ichihara, Y., Nakamura, N, Nabeshima, K., Choi, B. and Nishida, A. (2022). *Applicability of Equivalent Linear Three-Dimensional FEM Analysis for Reactor Building to Seismic Response of SSI System*, SMiRT26 Conference, Special Session on Nonlinear Seismic SSI Analysis Based on Best Practices in US and Japan, Berlin, July 10-15

JEAC 4016-2015, Nuclear Standard Committee of Japan Electric Association (2015), *Technical Code for Aseismic Design of Nuclear Power Plants, Japan Electric Association*

Nitta, Y., Ikeda, R., Horiguchi, T. and Ghiocel, D.M. (2022). *Comparative Study Using Stick and 3DFEM Nonlinear SSI Models per JEAC 4601-2015 Recommendations*, SMiRT26, Special Session on Nonlinear Seismic SSI Analysis Based on Practices in US and Japan, July 10-15

Ozaki, M., Akita, S., Oosuga, H., Nakayama, T., Adachi, N. (2004). "Study on Steel Plate Reinforced Concrete Panels Subjected to Cyclic In-Plane Shear." *Nuclear Engg. and Design*, Vol. 228, pp. 225-244.

Varma, A., Malushte, S.R. Sener, K.C., Booth, P.N , Coogler, K.(2011). *Steel-Plate Composite (SC) Walls: Analysis, Design Including Thermal Effects,* SMiRT21, Div-X: Paper ID# 761, New Delhi, India,6-11 November